25th ABCM International Congress of Mechanical Engineering
October 20-25, 2019, Uberlândia, MG, Brazil

COB-2019-1419
A CONTRIBUTION TO ELECTROCHEMICAL NANOINDENTATION TECHNIQUE

José Eduardo Silveira Leal
Teófilo Jacob Freitas e Souza
Sinésio Domingues Franco
Vera Lúcia D. S. Franco
Rosenda Valdés Arencibia
Universidade Federal de Uberlândia, Av. João Naves de Ávila, 2121, Santa Mônica, 38400-902, Uberlândia - MG
joseleal@ufu.com.br; teofilojacob@gmail.com; sdfranco@ufu.br; vlfranco@ufu.br; rosenda.arencibia@ufu.br

Marcelo Torres Piza Paes
Petrobras, Centro de Pesquisas e Desenvolvimento Leopoldo Américo M. de Mello, Cidade Universitária, 21941-915, Rio de Janeiro - RJ
mtpp@petrobras.com.br

Abstract. *This study aims to adapt a nanoindentation tester (NHT^2) for performing the evaluation of the Inconel 718 hydrogen embrittlement (HE). This adaptation is necessary to investigate the effect of the hydrogen charging on the nanohardness (HIT) values, plane strain modulus (E*) and indentation depth (hm) of Inconel 718. For this purpose, nanoindentations were performed in an Inconel 718 sample. The hydrogen charging was carried out by cathodic protection with the sample immersed in a NaCl 3.5 % aqueous solution. The potential in the sample was applied using a three-electrode configuration. An Ag/AgCl standard reference electrode was used. The sample was charged under a potential of – 1.2 V. The hydrogen charging produced statistically significant effects on maximum indentation depth and nanohardness values of the Inconel 718 sample for a 95 % confidence level, whereas there was not significant change in E* average values. The hydrogen charging increased HIT average values by 19.3 % and 15.3 % for loading rates of 15 mN/min and 480 mN/min, respectively. The hm average values were reduced in 6.1 % and 7.8 %. The Inconel 718 alloy was susceptible to HE for the evaluated experimental conditions.*

Keywords: *electrochemical nanoindentation, hydrogen embrittlement, Inconel 718, calibration, acoustic enclosure.*

1. INTRODUCTION

Among the chemical elements, hydrogen has the smallest atomic diameter and, consequently, presents high mobility on solid materials. It diffuses easily through the material, changing the binding energy between the metal atoms and that may lead to the hydrogen embrittlement. However, because of the relatively low diffusion rate and high solubility of hydrogen in austenite, it is nearly impossible to achieve a uniform hydrogen concentration in a macroscopic sample at room temperature.

Electrochemical nanoindentation (ECNI) introduces the possibility of simultaneous electrochemical hydrogen charging and nanomechanical testing within a very small volume close to the surface, where the hydrogen concentration becomes uniform within a very short time (Asgari; Johnsen; Barnoush, 2013). The combination of nanoindentation with an electrochemical cell enables the study of local dislocation mechanisms and opens up the possibility of investigating the hydrogen/deformation interaction on the nanoscale (Barnoush and Vehoff, 2006a, 2006b).

During nanoindentation tests, a known force is applied, whereas the resulting penetration depth is recorded. The force plot as a function of the penetration depth is used to evaluate the mechanical response of the material. The validation of the nanotest results in materials oil and gas field undergoes extensive experimentation. Thus, this study aims to adapt a nanoindentation tester (NHT^2) for performing the evaluation of the Inconel 718 hydrogen embrittlement.

2. EXPERIMENTAL PROCEDURE

A nanohardness tester (NHT^2) manufactured by Anton Paar was used (Fig. 1a). This equipment has a resolution of 20 nN for the force range from 0.1 mN to 500.0 mN, whereas for the indentation depth range from 20 nm to 200 μm the resolution is of 0.01 nm. The NHT^2 has a Berkovich B-Y 00 diamond tip indenter with $\alpha = 65.3 \pm 0.3°$ edge angle, two

ruby reference balls (Fig. 1b) and a liquid container (Fig. 2). The NHT^2 operation for the in situ evaluation of the susceptibility to HE requires the execution of three main steps, described below.

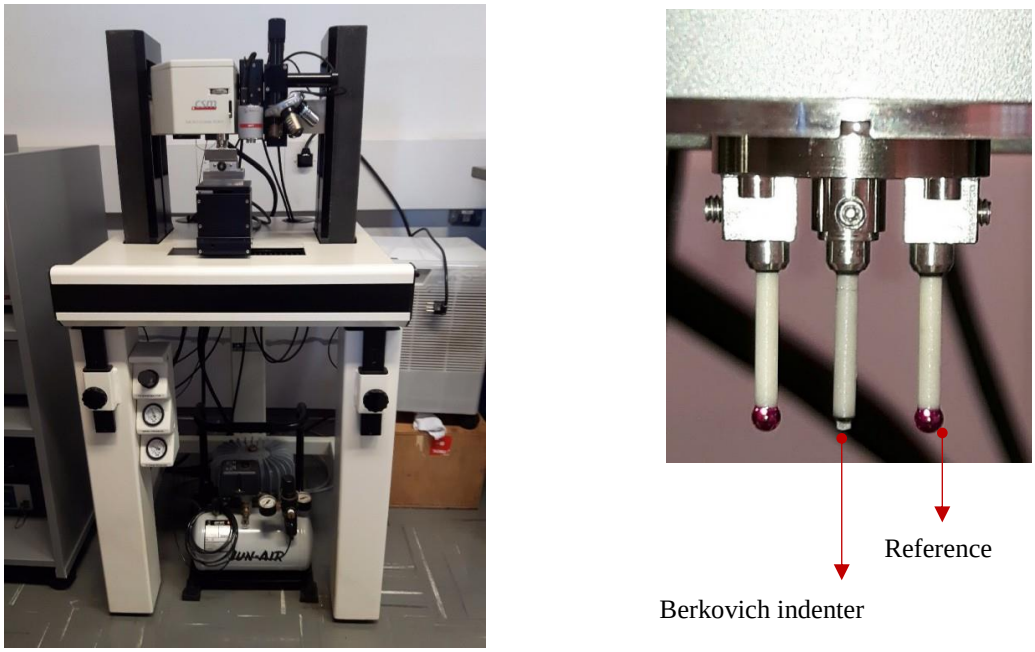

Figure 1. a) Nanohardness tester NHT^2 and b) Berkovich indenter and reference balls.

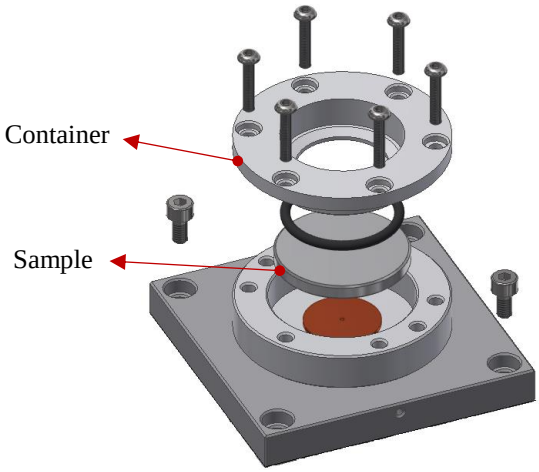

Figure 2. Electrolyte container.

2.1 NHT^2 indenter calibration

The indenter calibration consisted of indirectly measuring a projected area *Ap* using the plane strain modulus (*E**) value of a fused silica sample. The silica sample calibration certificate declares an *E** of 75.3 ± 0.3 GPa. For calibration purposes, 110 indentations were carried out on the sample. The minimum applied force was 0.1 mN and it was incremented every 5 indentations until the maximum force of 100 mN. Prior to the tests, the indenter and the silica sample were maintained at room temperature of 20.0 ± 1.0 °C for 8 h.

During the indenter calibration, it was observed that several curves of Force, *F*, per indentation depth, *h*, (*F*-*h* curves) showed different shape than the typical one, expected for the nanohardness measurement. Figure 3a shows a typical *F*-*h* indentation curve performed using 0.1 mN force. The observed errors were attributed to mechanical vibration transmitted through to the ground and air, and noises in the electric network. Moreover, at 10 mN (Fig. 3b) a significant increase in the *h value* was observed without any increase of *F* at the beginning of the indentation test indicating that the equipment started in the loading cycle without the indenter being in contact with the sample. In this way, the contact between the indenter and the sample was detected prematurely and the loading cycle was anticipated.

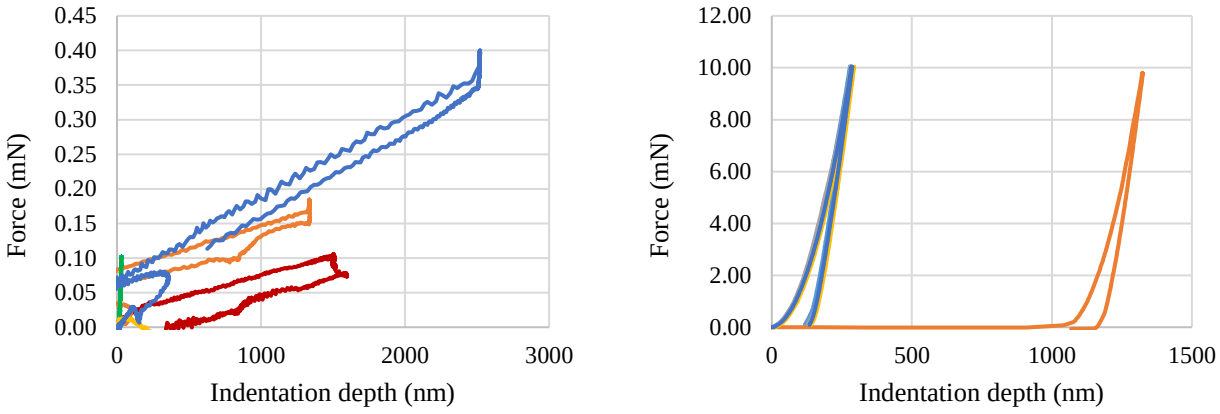

a) b)

Figure 3. *F-h* curves obtained during NHT^2 indenter calibration at a) 0.1 mN, and b) 10 mN.

In order to reduce the effect of the identified error sources, an acoustic enclosure (Fig. 4) with a 1500 × 820 × 820 mm^3 was designed and manufactured. Galvanized plain sheets with 1.2 mm thickness were used for the cabin outer and inner wall. The space between the outer and inner walls was filled up with a 64 kg/m^3 density rockwool insulation sheets. To the rockwool sheets was added a single face coating composed of aluminum foil bonded to kraft paper with flame retardant adhesive and reinforced with three-way glass fiber (FSK coating). In addition, the indentations were performed during off peak hours.

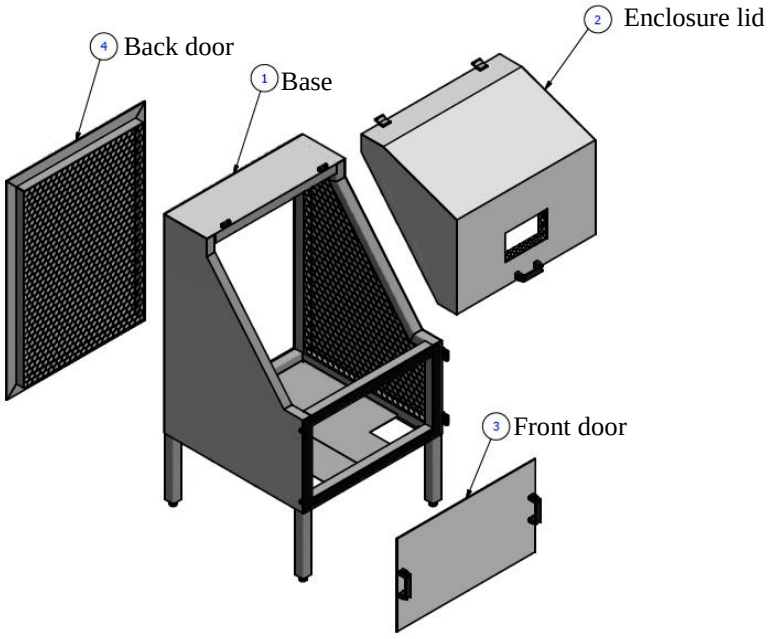

Figure 4. Acoustic enclosure for NHT^2.

The noise level in the room and inside the cabin was evaluated using the SmartdB® audiodosimeter manufactured by Chrompack Instrumentos Científicos Ltda. This instrument belongs to accuracy class 1 in accordance with ABNT NBR IEC 61672-3 (ABNT, 2018) standard. Two experiments were performed, in the first the audiodosimeter was positioned outside the cabin, Fig. 5a. During the second, the audiodosimeter was positioned inside the cabin, Fig. 5b. For both experiments, a sampling time of 14 h was established.

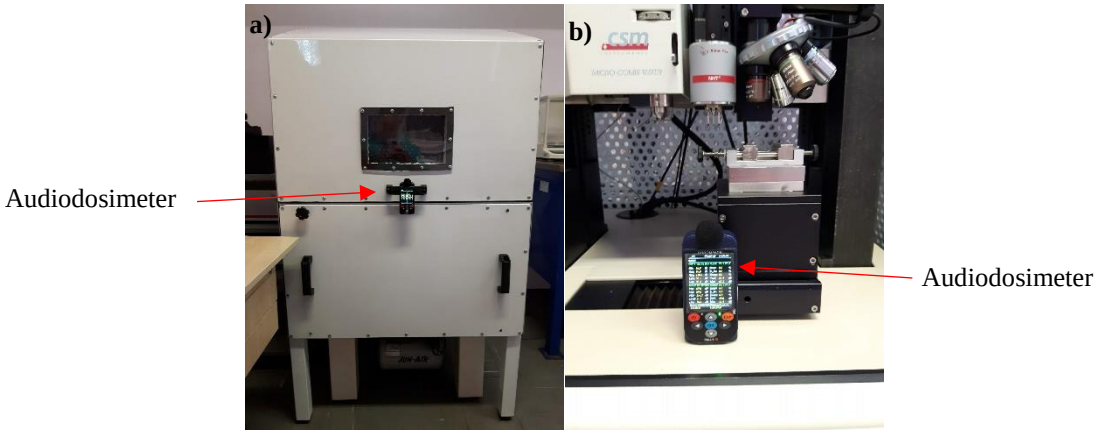

Figure 5. a) Audiodosimeter outside the enclosure and b) inside the enclosure.

In order to assess the NHT^2 accuracy, a verification test was conducted on the silica sample. The maximum force applied was 80 mN, loading and unloading rate were 160 mN/min and pause of 30 seconds at the maximum force. The E^* results should be in the range of the value given by the certificate ± 5 %.

2.2 Electrochemical cell

For the hydrogen charging, a voltage source, an external voltmeter, a platinum wire counter electrode (CE), an Ag/AgCl reference electrode (RE), and the sample acting as the work electrode (WE) were used (Fig. 6a).

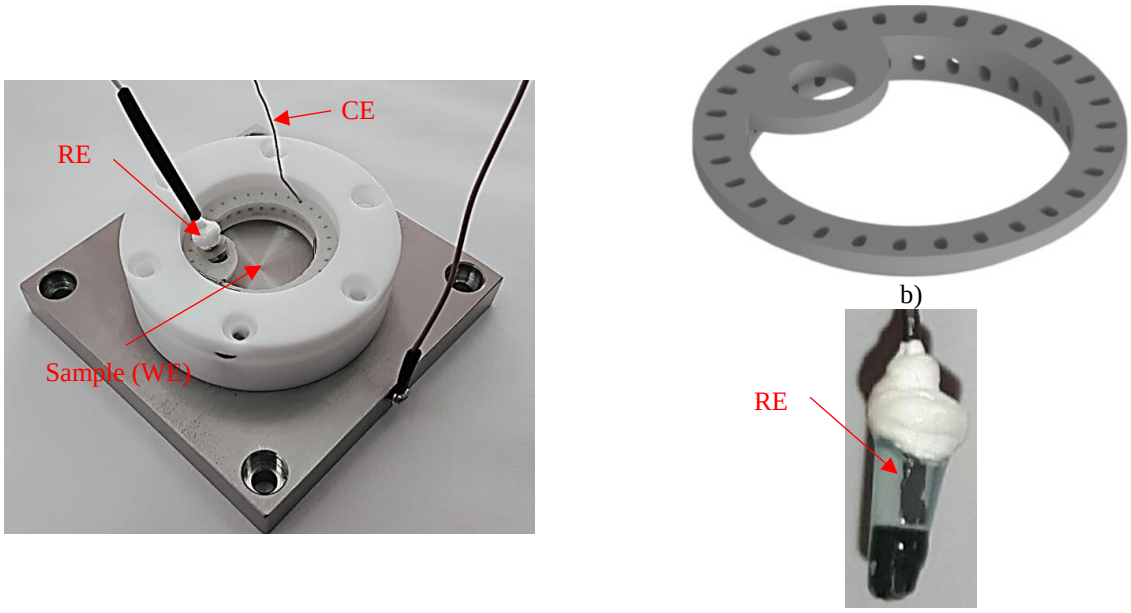

Figure 6. a) Electrochemical cell, b) electrode holder and c) Ag/AgCl electrode.

In order to couple the Ag/AgCl electrode and the platinum electrode to the NHT^2 liquid container, an electrode holder (Fig. 6b) was designed and manufactured. For this purpose, 3D printing of acrylonitrile butadiene styrene (ABS) was used. A miniaturized RE was fabricated using a 99 % silver wire, a pipette tip and a microporous membrane (Fig. 6c). To get an Ag/AgCI RE, a silver wire must first be covered with an AgCl layer. Thus, the silver wire was placed under anode potential of + 0.3 VAg/AgCl in a solution of 0.1 molar HCl for two hours.

2.3 ECNI tests

Prior to the tests, the electrochemical cell and the long shat indenter were cleaned in isopropanol and exposed to room temperature of 20.0 ± 1.0 °C for 8 hours. A clean tip shaft reduces the capillary forces acting on it (Asgari et al., 2012). Afterwards, an indentation at 50 mN in a copper sample was performed to remove remaining dirt.

The Inconel 718 alloy tested in this work was aged in two steps: 8 h at 718 °C, cooled to 621 °C and held for 10 h before air cooling at room temperature. An Inconel 718 sample with 4 mm thickness and 35 mm diameter was manafuctured by electrical discharge machining. The sanding and mechanical polishing of the sample surface were carried out using 220, 500 and 1200 mesh sanding papers and abrasives of 6 µm, 3 µm, 1 µm and 40 nm colloidal silica, respectively.

The sample roughness *Ra* (arithmetical mean deviation of the assessed profile) was measured using an interferometer in white light mode (CLA). This equipment has a vertical resolution of 0.01 µm. Measurement management and data recording were performed through the Talysurf CLI 2000® software. The calibration certificate states an expanded uncertainty of 0.05 % associated with the interferometer calibration, for a coverage factor *k* of 2.00 and a coverage probability of 95 %. Five measurement cycles were performed. A 0.25 mm sampling length was defined based on ISO 12085 (2013) Standard. The evaluation length was 1.25 mm. The Gaussian filter was applied on the primary extracted profile.

For the hydrogen charging a cathodic potential of -1.2 $V_{Ag/AgCl}$ was applied at the sample immersed in a 3.5 % NaCl aqueous solution in a three-electrode configuration (Fig. 7). Indentations without hydrogen charging were performed prior to electrolyte insertion. Afterwards, the electrolyte was inserted and the potential of -1.2 $V_{Ag/AgCl}$ was maintained for one hour before the electrochemical nanoindentations start to ensure the hydrogen charge.

During the indentations, the reference electrode was removed and the potential between the WE and EC was kept constant and equal to the potential between these electrodes when the RE was still present. The reference electrode may be removed since periodic electrical potential checks are made reinserting the RE into the cell. The electrical potential difference between the WE and the RE remained constant after the removal of the Ag/AgCl reference electrode, no need for corrections at this potential during the execution of the tests.

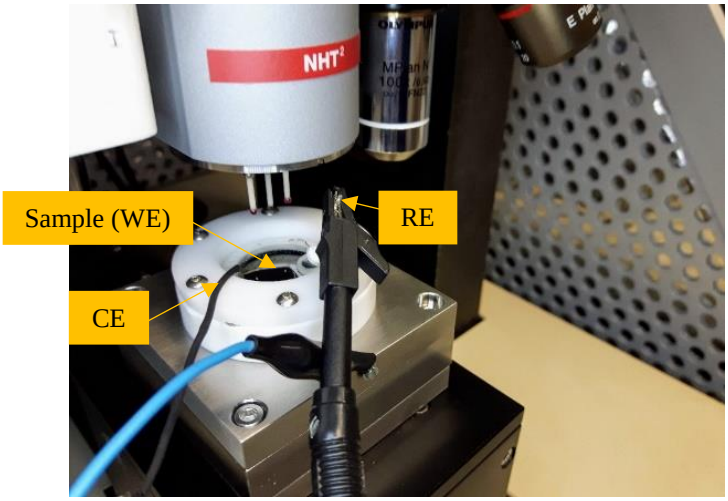

Figure 7. Sample immersed in a 3.5 % NaCl aqueous solution in a three-electrode configuration.

In order to investigate the effect of the hydrogen charging on the Inconel 718 nanomechanical properties, 40 nanoindentations were performed on the sample, see Tab. 1.

Table 1: Experimental design.

Condition	Hydrogen charging	Loading rate	Indentations
1	-1 (air)	-1 (15 mN/min)	10
2	-1 (air)	1 (480 mN/min)	10
3	1 (-1.2 V)	-1 (15 mN/min)	10
4	1 (-1.2 V)	1 (480 mN/min)	10

For conditions 1 and 3, the load function of each indentation consists of a loading rate of 15 mN/min up to the maximum force of 2.5 mN. Here the force was kept constant for 10 s before a reduction to 0 mN at a rate of 15 mN/min. The Approach speed was 1000 nm/minute, the retract speed was 2000 nm/minute and the acquisition rate was 10 Hz. On

the other hand, for conditions 2 and 4, the load function of each indentation consists in a loading rate of 480 mN/min up to the max load of 2.5 mN and the force is kept constant for 2 s before a reduction to 10 % of the maximum load at a rate of 480 mN/min. Finally, the load is kept at 10 % of the max load for 1 s for drift correction.

The nanohardness, the plane strain modulus, the maximum indentation depth and the force graph as a function of the penetration depth were collected from each experiment. The analysis of the results was conducted using the Statistica 7.1 software.

According to Barnoush and Vehoff (2010), there are additional concerns that arise when indenting in a liquid environment due to the capillary and buoyancy forces acting on the tip. These authors also described one way to avoid this problem: for this purpose, the surface is first engaged with a higher set point of contact force. The tip is then moved a few nanometers away from the surface and the forces on the tip balance, while it rests above the surface. After this procedure, the surface can be easily engaged as usual.

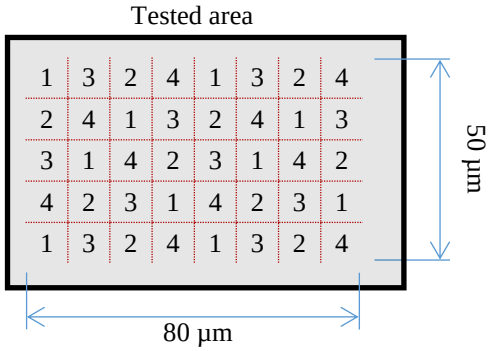

Figure 8. Randomized indentations map.

The indentation map was generated in order to minimize the confounding of possible nanohardness variations in the tested area with the effect of the hydrogen charging and loading rates. Thus, the position of each indentation and its replicas was defined as shown in Fig. 8. In this figure, numbers 1-4 indicate the test conditions.

3. RESULTS AND DISCUSSION

3.1 NHT^2 indenter calibration

Figure 9 shows the acoustic attenuation for equivalent continuous sound pressure level (LEQ) per octave band.

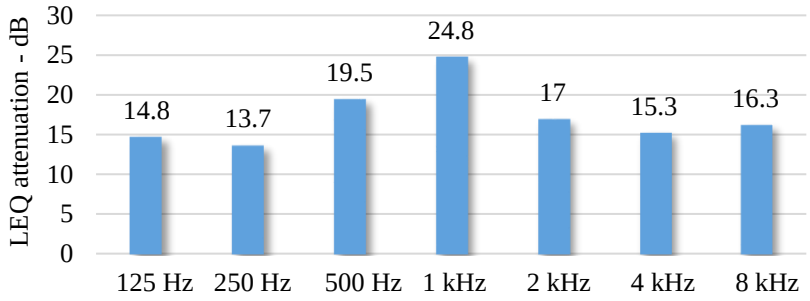

Figure 9. Differences between equivalent continuous sound pressure level in the room and inside the acoustic enclosure.

In Fig. 9 it was observed that the installation of the acoustic enclosure promoted a maximum attenuation of 24.8 dB at 1 kHz and a minimum of 13.7 dB at 250 Hz. Therefore, a reduction in the vibration effects on the investigated parameters noise is expected.

Figure 10 shows the *F-h* curves resulting from the indenter calibration at the maximum force of 0.1 mN. It was observed that the curves showed an expected shape for the instrumented indentation testing even when the force applied was equal to the lower limit of the equipment nominal range. This result confirms that the acoustic enclosure contributed to the noise reduction in *F-h* curves.

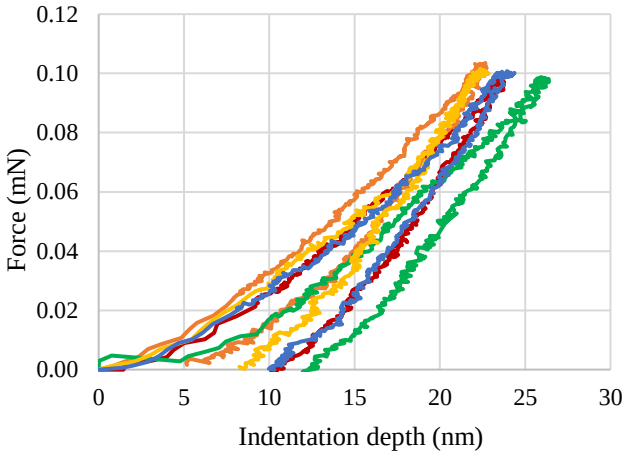

Figure 10. *F-h* curves resulting from NHT^2 indenter calibration at the maximum force of 0.1 mN.

Table 2 shows the silica plane strain modulus (*E**) measured values after indenter calibration.

Table 2. Measurement results of silica sample plane strain modulus (*E**).

Indentation	***E**** **(GPa)**
1	75.226
2	75.703
3	75.189
4	75.571
5	75.552
Average	75.448
Standard deviation (68.27 %)	0.228

The silica sample *E** showed an average value of 75.448 GPa with an associated standard deviation of 0.228 GPa, for a confidence interval of 68.27 % (Tab. 2). This result shows that NHT^2 accuracy was in accordance with the manufacturer specification (± 5 %).

3.2 ECNI tests

Figure 11 shows a roughness profile obtained by white light interferometry on the surface of the Inconel 718 sample.

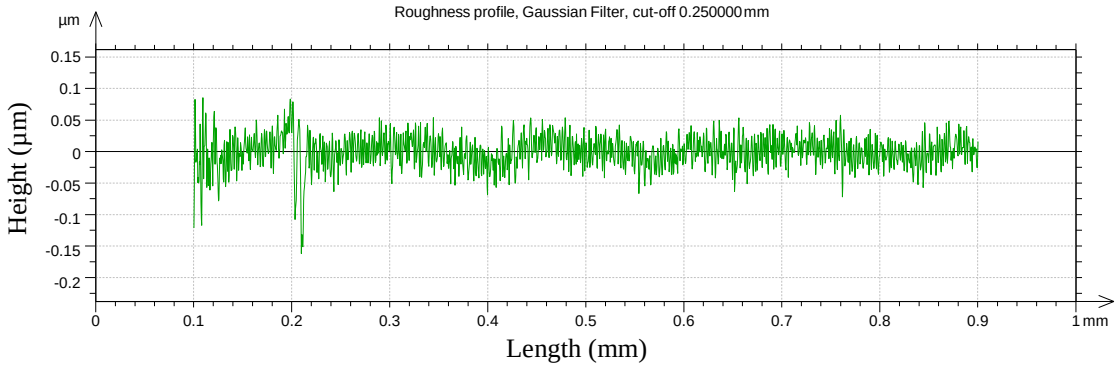

Figure 11. Roughness profile obtained on Inconel 718 sample.

The average *Ra* of the Inconel 718 sample was 0.02 µm and the standard deviation was 0.01 µm for a confidence interval of 68.27 %. In this case, as recommended by the NHT^2 manufacturer, in order to reduce the nanohardness variability, the minimum penetration depth should be at least 400 nm. However, the ECNI tests were performed with penetration depths nearly to 120 nm. The sample surface finish may have contribute to the nanohardness variability.

Figures 12a and 12b show the *F-h* curves resulting from nanoindentation tests using loading rate of 15 mN/min and 480 mN/min, respectively. According to Figs. 12a and 12b, with the hydrogen charging, a decreasing trend of *hm* and an increasing trend of *HIT* were observed. These results are corroborated by those shown in Fig. 13 and in Tab. 2.

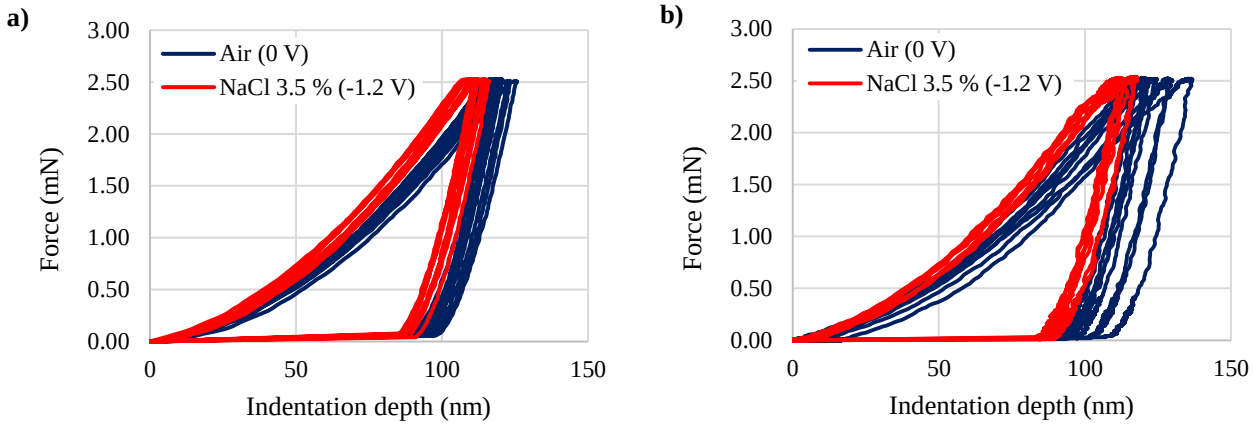

Figure 12. a) *F-h* curves with and without hydrogen charging at 15 mN/min, and b) *F-h* curves with and without hydrogen charging at 480 mN/min.

Figures 13a, 13b and 13c show the average values and confidence intervals (95 %) of *hm*, *HIT* and *E**, respectively. In these figures, the effect of the hydrogen charging on the values of the evaluated parameters can be visualized. It was observed a decrease of *hm* and an increase of HIT with the hydrogen charging. There were no significant effects of hydrogen charging on *E** values.

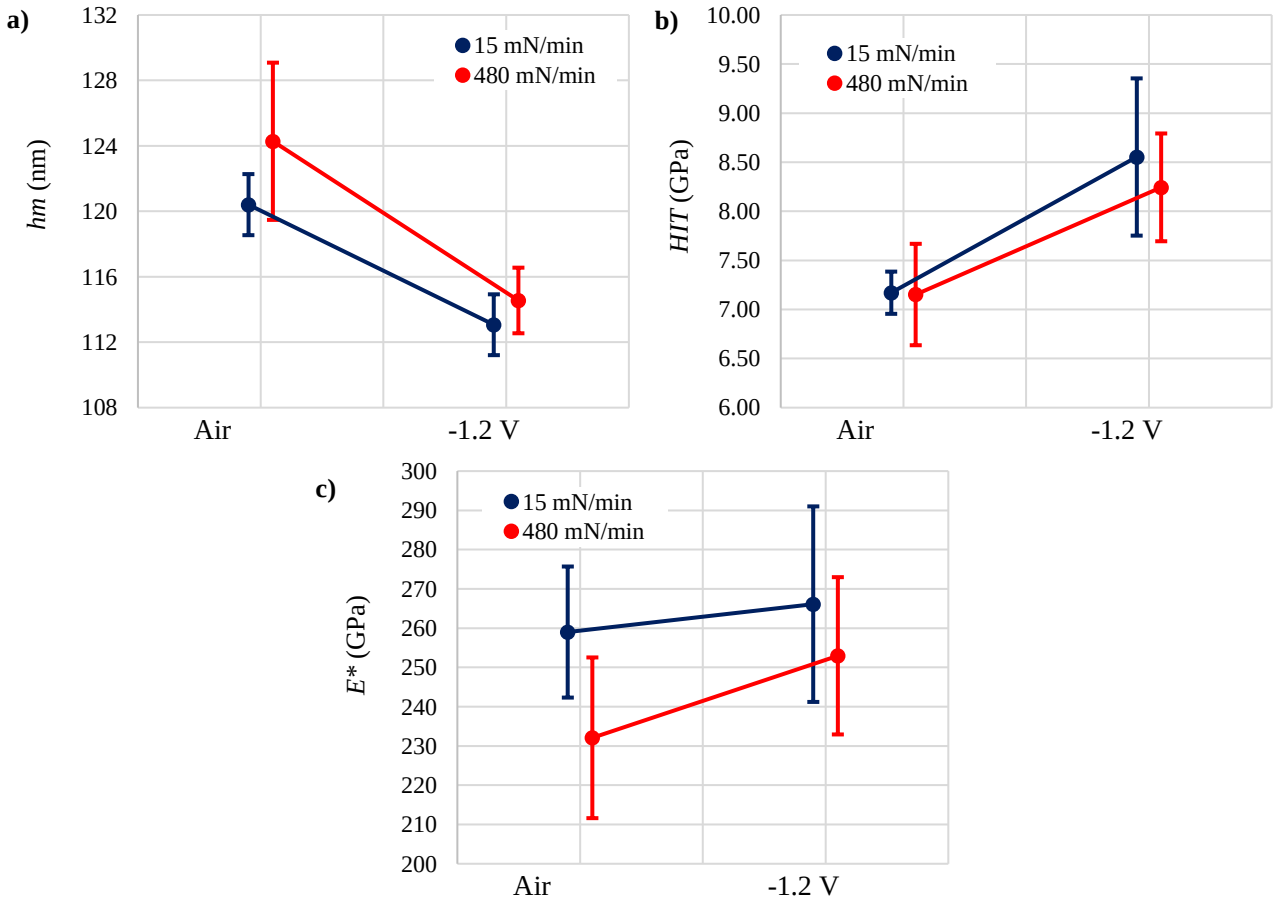

Figure 13. Average values and weighted confidence intervals (95 %) of *hm*, *HIT* and *E** obtained in the ECNI test

In Table 3 it was observed that the *p-values* lower than 0.05 were obtained for "1 and 3" and "2 and 4" groups for *hm* and *HIT*. This indicates that hydrogen charging resulted in significant changes in Inconel 718 nanomechanical properties for both loading rates. On the other hand, the *p-values* obtained for "1 and 2" and "3 and 4" groups show that the loading rate did not lead to changes in *hm* and *HIT* values. For the plane strain modulus (*E**), there was no significant changes induced by hydrogen charging and the "1 and 2" *p-value* indicating that loading rate can influence *E** values. These results suggest a relation between *E** and the loading rate.

Table 3. Results obtained from the Student's t-test

Groups	***hm***	***HIT***	***E****
		p-value	
1 and 2	0.1147	0.9414	0.0330
1 and 3	0.0000	0.0048	0.5825
1 and 4	0.0002	0.0023	0.5916
2 and 3	0.0005	0.0047	0.0256
2 and 4	0.0015	0.0040	0.1057
3 and 4	0.2093	0.4523	0.3355

It can be concluded that the hydrogen charging in the Inconel 718 sample resulted in an increase of the nanohardness and a reduction of the maximum indentation depth. Hence, it was found that, for the evaluated experimental conditions, the Inconel 718 alloy was susceptible to HE.

4. CONCLUSION

a) The indenter calibration showed that the mechanical vibration transmitted through to the ground and air can affect the *F-h* curves with forces lower than 10.0 mN. Incorrect detection of the indenter-to-sample contact point represents a significant error source.
b) The acoustic enclosure installation contributed to attenuate the effects of airborne vibration related errors.
c) Hydrogen charging by cathodic protection produced statistically significant effects on *hm* and *HIT* values considering a confidence level of 95 % in the Inconel 718 sample. The average value of the *HIT* was increased by 19.3 % and 15.3 % in the presence of cathodic protection for 15 mN/min and 480 mN/min, respectively. In turn, the *hm* average values were reduced by 6.1 % and 7.8 % for 15 mN/min and 480 mN/min, respectively. There was no significant change in *E** values with hydrogen charging.
d) For the conditions of this experiment, the Inconel 718 alloy was susceptible to hydrogen embrittlement.

5. ACKNOWLEDGEMENTS

This work was supported by CAPES-PROEX and PETROBRAS.

6. REFERENCES

Associação Brasileira De Normas Técnicas, 2008. ABNT NBR ISO 4288: Especificações geométricas do produto (GPS) — Rugosidade: Método do perfil — Regras e procedimentos para a avaliação da rugosidade.

Associação Brasileira De Normas Técnicas, 2018. ABNT NBR IEC 61672-3: Eletroacústica — Sonômetros Parte 3: Testes periódicos.

Asgari, M.; Johnsen, R.; Barnoush, A., 2013. "Nanomechanical characterization of the hydrogen effect on pulsed plasma nitrided super duplex stainless steel". *International Journal of Hydrogen Energy*, v. 38, n. 35, p. 15520–15531.

Barnoush, A.; Vehoff, H., 2006a. "Electrochemical nanoindentation: A new approach to probe hydrogen/deformation interaction". *Scripta Materialia*, v. 55, n. 2, p. 195–198.

Barnoush, A.; Vehoff, H., 2006b. "In situ electrochemical nanoindentation of a nickel (111) single crystal: hydrogen effect on pop-in behavior". *International Journal of Materials Research*, v. 97, n. 9, p. 1224–1229.

Barnoush, A.; Vehoff, H., 2010. "Recent developments in the study of hydrogen embrittlement: Hydrogen effect on dislocation nucleation". *Acta Materialia*, v. 58, n. 16, p. 5274–5285.

International Organization for Standardization, 2013. ISO 12085:1996 - Geometrical Product Specifications (GPS) -- Surface texture: Profile method -- Motif parameters.

7. RESPONSIBILITY NOTICE

The authors are the only responsible for the printed material included in this paper.